Journal of Nanoscience and Technology 2(2) (2016) 81–84

ISSN: 2455-0191

Contents List available at JACS Directory

Journal of Nanoscience and Technology

journal homepage: www.jacsdirectory.com/jnst

Investigation of Surface Plasmon Resonance and Optical Band Gap Energy in Gold/Silica Composite Films Prepared by RF-Sputtering

A. Belahmar[1], A. Chouiyakh[2,*]

Department of Physics, Laboratory of Condensed Matter Physics, Faculty of Science, IBN Tofail University, B.P.133, 14000, Kenitra, Morocco.

ARTICLE DETAILS

Article history:
Received 28 January 2016
Accepted 08 February 2016
Available online 03 March 2016

Keywords:
Au Nanoparticles
Silica Films
Surface Plasmon Resonance
Sputtering

ABSTRACT

Silica films containing gold nanoparticles were grown by magnetron radio frequency (rf) sputtering technique under various deposition conditions. XRD measurements revealed the formation of gold nanoparticles embedded in amorphous silica films. The structural and optical properties of the films were tailored by varying the system pressure and the sputtering area ratio of Au/SiO_2 for the target (r_{Au/SiO_2}). No apparent surface plasmon resonance peak was observed for the lower area ratio. An anomalous blue shift in peak position of SPR band absorption with the increase of gold nanoparticles size is observed. The peak wavelength of the surface plasmon resonance (SPR) was found to redshift from 500 nm to 510 nm, while the size decreases from 2.5 nm to 2.10 nm and disappears for the size lower than 2 nm. This composite exhibits the optical features of a semiconductor with direct band gap. The band gap energy of 3.45 eV and 4 eV achieved for gold nanoparticles when the area ratio decreases of 2.6% to 1.6% respectively.

1. Introduction

In recent years, an increasing understanding of nanocomposite material's behaviors has driven scientific and technological interest toward the fabrication of nanocomposite films containing noble metal nanoparticles (NPs) embedded in dielectric materials [1-4]. One of the most important aspects at the nanoscale is that the noble metals like silver and gold exhibit strong absorption in visible range. This absorption is known as the surface plasmon resonance (SPR). The origin of this absorption is attributed due to their collective oscillation of conduction band electron in response to the electrical field of the electromagnetic radiation of light [5, 6]. The SPR is a unique physical phenomenon only for nano-size particles, it is absent at scales of atoms or bulk [5, 7].

Recently, one of the main challenges in the study of noble metal dielectric system is the proper selection of the size and shapes of the noble metal particles in the dielectric matrix, which can lead to the control of surface plasmon resonance (SPR) peaks. Due to this, noble metal nanoparticles find a wide range of broad potential applications [8-10]. For their applications in nanotechnology, it is very important to controllably tune the surface plasmon resonance (SPR) wavelength of metal nanoparticles, which depends on the size and shape of nanoparticles, volume fraction of the metal in the nanocomposite, dielectric properties of the metal and the embedding matrix [11-15]. Manipulation of the position and intensity of the SPR peaks can be applied in industrial applications such as solar cell technology [16].

Parallel to the experimental efforts, many theories were developed in describing the optical responses from noble metal nanoparticles. The theoretical predictions are found to be in good agreement with experimentally measured spectra and can be used to interpret the optical effects observed during synthesis. Among the all existing theories, the M–G effective medium theory is the most comprehensive one [17]. It includes the contributions from the dielectric properties of both the particles and the matrix, the shape of the individual particles, and the particle-particle interactions. Under the mean field approximation, the optical property of the nanocomposite system is described by as ε_{eff} a whole, which is the dielectric function of the effective medium which satisfies the equation [18].

$$\frac{\varepsilon_{eff}-\varepsilon_m}{\varepsilon_{eff}+2\varepsilon_m}=q\frac{\varepsilon-\varepsilon_m}{\varepsilon+2\varepsilon_m} \quad (1)$$

Where q is the volume fraction of the metallic particles, ε is the dielectric function of the metallic particles and ε_m is the dielectric function of the matrix. The dielectric function of Au was taken from the work of Palik [19]. The dependence of the metal dielectric function on the size of the particles is taken into account using the model presented by Hövel et al [20]:

$$\varepsilon(\lambda, D) = \varepsilon^{bulk}(\lambda) + \frac{\omega_P^2}{\omega^2 + i\omega\gamma_{bulk}} - \frac{\omega_P^2}{\omega^2 + i\omega(\gamma_{bulk} + 2A\,v_F/D)} \quad (2)$$

Where ε is the bulk gold dielectric constant, ω_P, v_F and γ_{bulk} being, the metal plasma frequency, the Fermi velocity and the electron scattering rates in the bulk respectively, and A is a phenomenological parameter including details of the scattering process. The absorption coefficient α of the composite can be obtained from the following formula [21]:

$$\alpha = \frac{4\pi}{\lambda\sqrt{2}}\left[(\varepsilon_{e1}^2 + \varepsilon_{e2}^2)^{1/2} - \varepsilon_{e1}\right]^{1/2} \quad (3)$$

Where ε_{e1} and ε_{e2} are the real and imaginary parts of the effective dielectric function ε_{eff}.

Nanocomposite films consisting of metal particles such as gold embedded in a silica matrix have recently been the subject of many studies [22-35]. A large number of methods have been used to obtain AuNPs embedded in SiO_2 films, such ion implantation [36-37], sol-gel [38], plasma enhanced chemical vapor deposition (PECVD) [39], hybrid techniques combining pulsed-DC sputtering and PECVD, which is used for simultaneous Au sputtering and SiO_2 deposition [26, 27], and RF magnetron sputtering [22, 23, 28-32, 35, 40-42]. The flexibility and easy fabrication of diverse composite films are the advantages of sputtering method. The important factors to influence the formation of AuNPs are the working distance between the target and the substrate, rf-power, sputtering time, the temperature of the target, applied voltage, and working pressure.

The purpose of this work is to investigate the influence of gold-to silica surface ratio and deposition argon pressure on the structural and optical properties of gold nanoparticles embedded in silica films grown by RF-magnetron sputtering technique.

*Corresponding Author
Email Address: ali_chouiyakh@hotmail.com (Ali Chouiyakh)

Cite this Article as: A. Belahmar, A. Chouiyakh, Investigation of surface plasmon resonance and optical band gap energy in gold/silica composite films prepared by rf-sputtering, J. Nanosci. Tech. 2(2) (2016) 81–84.

2. Experimental Methods

The samples, consisting of gold/silica composite thin films, were prepared by conventional radio-frequency magnetron sputtering method using an Alcatel SCM 650 apparatus. The target is constituted by two materials: a silica disc with a diameter of 50 mm was used as a target, over which chips of gold covering a fraction of the target area (r_{Au/SiO_2}), were placed on top of silica disc. The deposition was accomplished on clean glass substrates at room temperature. The chamber was evacuated to a pressure better than10^{-6} mbar before the argon gas for the sputtering was introduced. Deposition was carried out at a pressure over the range $2x10^{-3}$– $5x10^{-3}$ mbar and the 1.3% -2.6% of gold/silica ratio, of materials from which the composite film is fabricated. All the deposition of the samples was performed at a fixed substrate to target distance of 60 mm. The deposition time and applied power were kept constant at 4 h 30 min and 50 W, respectively.

The structural characterization of the composite films was performed in a Philips PW 1710 spectrometer using Cu k_α radiation ($\lambda = 1.54056$ Å). The diffraction patterns were collected over the range 2θ = 10° to 80° at room temperature.

Optical absorption spectra, of Au/SiO_2 composite films, were registered by a Shimadzu UV 30101 PC spectrometer, in near ultra-violet-visible-near infra-red range (NIV-VIS-NIR) from 300 to 2000 nm.

3. Results and Discussion

3.1 Structural Characterization

The control particle size, particle shape and morphology are very much important in nanoparticles preparation. The most important tool to study the nanomaterials is X-ray diffraction.

Fig. 1 (b, c, and d) shows the XRD patterns of the Au/SiO_2 composite films deposited at various argon pressures and a fixed $r_{Au/SiO_2} = 1.3\%$. X-ray diffractogram of gold thin film with a cubic structure, presented as a reference, is also reported in Fig. 1(a). It is evident that there are no Bragg reflections that are clearly visible in the spectra, due to the small AuNPs. It can be seen that the spectra of all the samples had a peak centered on 2θ=26° corresponds to the amorphous silica.

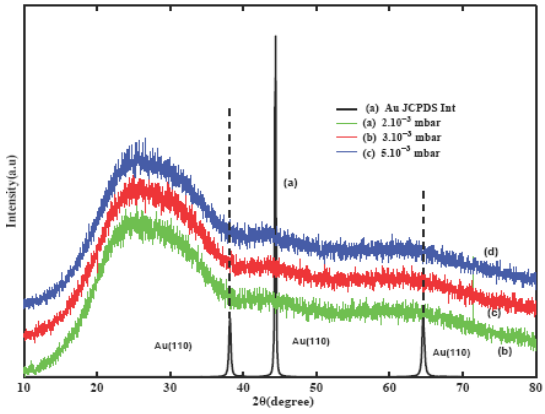

Fig. 1 Compare the XRD patterns of gold thin films and Au/SiO_2 composite deposited with different argon pressure and at fixed $r_{Au/SiO_2} = 1.3\%$

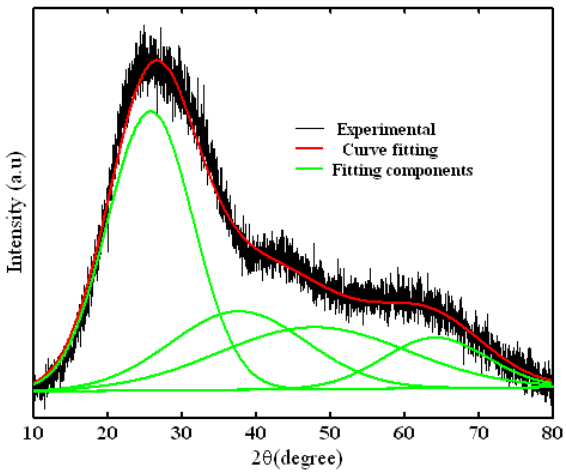

Fig. 2 Experimental diffractogram of the sample deposited at $2x10^{-3}$ mbar and their curve fitting where different pseudo-Voigt functions were taken into account.

The XRD spectra did not exhibit a significant change, indicating that the average size of AuNPs does not vary considerably under this deposition conditions. To determine the phase structure, size and lattice constant of AuNPs embedded in silica films, deconvolution procedure was used where details are reported elsewhere [28, 43].

The curve fitting of the XRD spectrum of the sample deposited at 0.002 mbar is reported in Fig. 2. Outside the peak assigned to silica matrix, the diffraction peaks resulting from the fitting are attributed to the crystal planes of (111), (200) and (220). Table 1 summarizes the fitting parameters determined from the Au (111) orientation plane for all the samples. From the values of the Bragg angle position and the full width at half maximum (FWHM) of the dominant peak Au (111) reflection, we estimated the particle size (D) using the Debye-Scherrer's equation [44]:

$$D = 0.9\lambda/(FWHM)\cos\theta_B \qquad (4)$$

Where λ is the wavelength of X-ray $(1.54056\ Å)$ and θ_B the Bragg diffraction angle. The average size was found to be in the range $0.38 - 0.40$ nm. We concluded that the pressure argon did not exhibit a significant change on the average size of AuNPs. However, another series of samples was deposited with the same preceding pressures argon but at fixed $r_{Au/SiO_2} = 2.6\%$. Fig. 2(a, b, c) shows the XRD patterns of the samples.

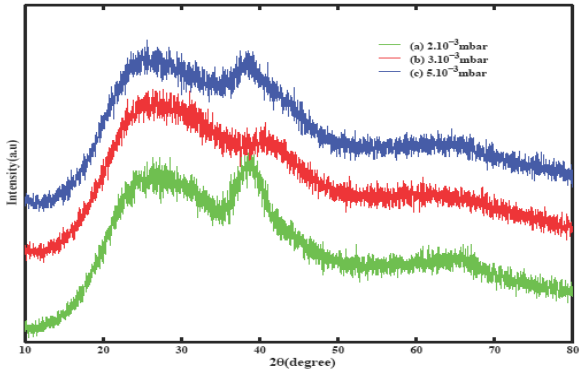

Fig. 3 XRD spectra of the Au/SiO_2 composite films deposited at different argon pressure and at fixed $r_{Au/SiO_2} = 2.6\%$

The deconvolution procedure of the XRD spectra was undertaking. The comparison of the three peaks with a JCPDS–04–0784 database are attributed to (111), (200), and (220) reflections of the fcc structure of Au nanocrystal. We can note that the intensity of the Au diffraction peaks increases with decreasing the argon pressure. The argon pressure influences the size of AuNPs in two opposite aspects. On the one hand, the average size decreases from 1.14 nm to 0.54 nm, with increasing argon pressure from $2x10^{-3}$ to $3x10^{-3}$ mbar; on the other hand, the size increases from 0.54 nm to 0.73 nm when the argon pressure changes from $3x10^{-3}$ to $5x10^{-3}$ mbar, indicating the existence of a critical pressure that separates the two opposite aspects. Belahmar et al [43] found also, that the argon pressure has the same effect in the case of gold nanoparticles in the size range 2.9-3.5 nm, embedded in alumina matrix grown by cosputtering. They attributed this phenomenon to the mean-free path of the sputtered species in the background argon gas. As argon pressure increases, the sputtered species undergoes a higher number of collisions; hence, fewer particles arrive at the substrate with the subsequent decrease in size of Au nanoparticles.

Table 1 Results of the curve fitting of the experimental diffractograms of the samples deposited with difference gold-to silica surface ratio and various argon pressures.

r_{Au/SiO_2}	Argon pressure (mbar)	FWHM (degree)	2θ (degree)	Lattice parameter (Å)	size (Å)
1.3%	$2x10^{-3}$	20.89	37.68	4.1315	4.02
	$3x10^{-3}$	25.56	38.32	4.0650	3.30
	$5x10^{-3}$	21.68	37.71	4.1283	3.87
2.6%	$2x10^{-3}$	7.42	38.68	4.0286	11.35
	$3x10^{-3}$	15.55	38.68	4.0286	5.41
	$5x10^{-3}$	11.48	38.61	4.0356	7.33

3.2 Optical Studies

Figs. 4 and 5 show the condition sputtering dependence of absorption spectra around the surface plasmon resonance (SPR) bands of AuNPs embedded in silica matrix. Comparing these results, remarkable differences in the spectra are observed. First, the spectra of AuNPs prepared at $r_{Au/S_iO_2} = 1.3\%$ (Fig. 4), have little or no plasmon bands. It is

well known that the peak position and absorbance of the SPR band depend on AuNPs' size. Namely, in the case of spherical AuNPs less than 2 nm in size, the plasmon band disappears [13, 45]. This is because the electron density in the conduction band becomes very small. Consequently, the number of electrons to be transferred to the surface plasmon state will reduce significantly and single electron excitations between the quantized energy levels will take place [46]. Instead of the collective oscillation of the electrons, plasmons will be confined to isolated ultrafine grains [47] and will be largely broadened and disappeared. This situation is depicted in Fig. 4. In contrast, in other spectra of AuNPs prepared at $r_{Au/S_iO_2} = 2.6\%$ (Fig. 5), we observe the noticeable SPR absorption band around 500 nm. For the sample grown at $2x10^{-3}$ mbar, the SPR band absorption is very distinct, while the plasmon band decreases in intensity, redshift and broadened substantially with increasing working argon pressure.

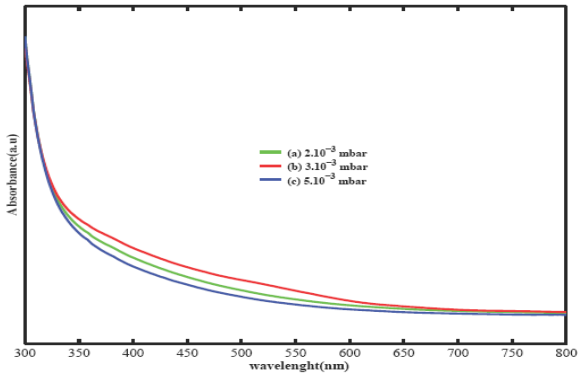

Fig. 4 Optical absorption spectra of Au/SiO_2 composite thin films deposited at different argon pressure and a fixed $r_{Au/S_iO_2} = 1.3\%$

Using M-G theory with mean free path correction, the theoretical absorption spectra were calculated by a combination of Eqs. (1), (2) and (3). We use for gold nanoparticles, the values of, $\omega_P = 1.39x10^{16}$Hz, $v_F = 1.4x10^6$ m/s, $\gamma_{bulk} = 1.1x10^{11}$ s^{-1} and a value for A = 2 [43] is required to extract the correct fitting parameters. These fittings allowed us to evaluate the Au particle size (D), the SPR wavelength λ_{max} the volume fraction of the metallic particles q and the dielectric function of the surrounding medium (ε_m) of each sample in the case of the samples deposited at $r_{Au/S_iO_2} = 2.6\%$. The simulation and the experimental plots are shown in Fig. 6 (a, b, c). The parameter values deducted from this simulation are summarized in Table 2.

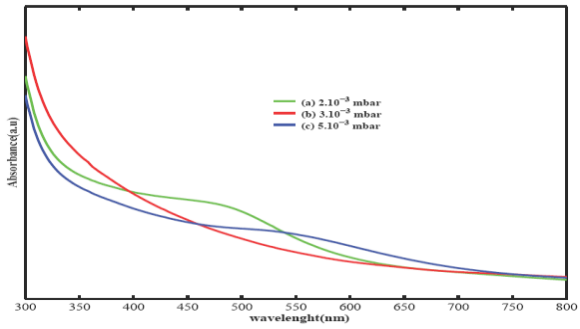

Fig. 5 Optical absorption spectra of Au/SiO_2 composite thin films deposited at different argon pressure and a fixed $r_{Au/S_iO_2} = 2.6\%$

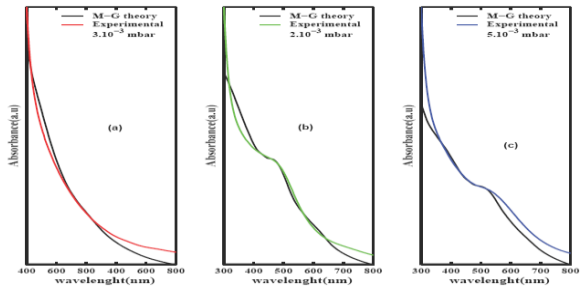

Fig. 6 Experimental and M-G simulated optical absorption spectra for the composites films deposited at argon pressures: $3x10^{-3}$ mbar (b) $2x10^{-3}$ mbar and (c) $5x10^{-3}$ mbar.

The plasmon peak positions just vary from 510 nm to 500 nm, and the size decreases slightly from 2.5 nm to 2.1 nm when the argon pressure increases from $2x10^{-3}$ mbar to $5x10^{-3}$ mbar and the SPR disappears for $3x10^{-3}$ mbar. This absorption band is consistent with the reported value for gold nanoparticles, where SPR appears around 500 nm [28]. The observed anomalous blue shift of the Au plasmon peak is not a new behaviour, it has been reported in the research work by Belahmar et al [43] .The appearance and disappearance of SPR in our samples suggests that there exists a critical particle size, argon pressure and metal concentration below which the surface plasmon resonance state is suppressed giving rise to a sharp absorption edge corresponding to semiconducting optical properties [48].

Table 2 Plasmon peak, average size, fraction volume dielectric functions of the surrounding medium of the sample deposited at 2.6% and various argon pressures.

r_{Au/SiO_2}	Argon pressure (mbar)	λ_{max} (nm)	Size(nm)	q %	ε_m
2.6%	$2x10^{-3}$	500	2.5	2	2
	$3x10^{-3}$	none	0.9	1	2
	$5x10^{-3}$	510	2.1	1.76	3. 7

The band gap energy can be determined using the Tauc relation. It is a convenient way of studying the optical absorption spectrum of a material. According to the Tauc relation, the absorption coefficient α for direct band gap material is given by [49],

$$(\alpha h\nu)^2 = A(h\nu - E_g) \qquad (5)$$

Where A is a constant, E_g is the optical gap expressed in eV and hν is the photon energy in eV. The band gap value E_g is determined by extrapolating the linear part of the $(\alpha h\nu)^2$ curve towards the hν axis until $(\alpha h\nu)^2 = 0$, as shown in Fig. 7. The obtained value of the optical band gap energy E_g are 3.85, 4.0 and 3.9 eV for the Au/SiO_2 nano-composite films deposited with $r_{Au/S_iO_2} = 1.3\%$ while the argon pressure increases from $2x10^{-3}$ to $5x10^{-3}$ mbar respectively. The E_g for the other series deposited at $r_{Au/S_iO_2} = 2.6\%$ in the same game of argon pressure are 3.4, 3.7 and 3.5 respectively. Note that the concentrations are 2%, 1% and 1.76%. It was observed that the E_g values decreased with the increase in fraction volume due to enlargement of nanoparticles size. However, Cai et al [48] reported that redshift of the absorption edge took place with Ag loading increasing from 0.75 wt% to 1.72 wt% in Ag/SiO_2 films, which was caused by simple scattering. There is a scattering dipole term as well as an absorption dipole term, which both contribute to the extinction. The redshift of the absorption edge with increasing Au content could also be attributed to an increase in scattering centres. Even if the particles grew with Au content, the scattering term in extinction would again increase giving rise to a redshift in the absorption edge. Our results are in agreement with those obtained by Z. Cui- Hua et al [51] who found also, in the case of Au/SiO_2 nano-composite thin films prepared by inductively coupled plasma sputtering, that band gap decreases with Au content increasing from 3 vol% to 37 vol %.

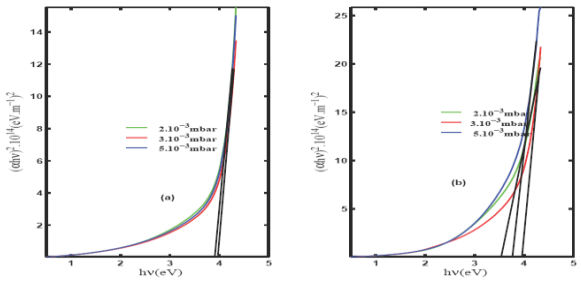

Fig. 7 Tauc plot of the sample deposited at different area ratio of Au/SiO_2 (a) 1.3%, (b) 2.6% and at different argon pressure

4. Conclusion

The sputtering area ratio of Au/SiO_2 for the target (r_{Au/SiO_2}) and argon pressure effect on the structural and optical properties of the gold nanoparticles dispersed in silica films grown by RF-magnetron sputtering were studied. The presence of small gold nanoclusters with size below 2 nm inside the silica matrix was confirmed by XRD and optical absorption measurements in the samples sputtered at $r_{Au/S_iO_2} = 1.3\%$ while the band gap edge is around the 4 eV. The sizes greater than 2 nm were found for the samples sputtered at $r_{Au/S_iO_2} = 2.6\%$ where the optical band gap energy is around the 3.5 eV. Both XRD and optical absorption measurements indicated a non-monotonic Au crystallite-size dependence of the argon pressure. The SPR absorption band exhibits an anomalous blue shift with increasing size. According to modified M-G theory taking

into account a correction of the dielectric constant for electron mean free path limitation, the plasmon band of gold clusters shifts from 500 nm to 510 nm.

Acknowledgments

We are grateful to Professor M.J.M. Gomes from the Centre of Physics, University of Minho, Portugal, for the experimental support.

References

[1] L. Armelao, D. Barreca, E. Bottaro, A. Gasparotto, S. Gross, C. Maragno, E. Tondello, Recent trends on nanocomposites based on Cu, Ag and Au clusters: A closer look, Coord. Chem. Rev. 250 (2006) 1294–1314.
[2] E. Céspedes, D. Babonneau, D.S. Meneses, C. Prietol, E. Fonda, O. Lyon, E. Briand, A. Traverse, Effects of Au layer thickness and number of bilayers on the properties of Au/ZnO multilayers, J. Appl. Phys. 109 (2011) 094308-094317.
[3] D. Buso, M. Post, C. Cantalini, P. Mulvaney, A. Martucci, Gold nanoparticle-doped TiO_2 semiconductor thin films: Gas sensing properties, Adv. Funct. Mater. 18 (2008) 3843-3849.
[4] K. Chan, Z. Aspanut, B. Goh, C. Sow, B. Varghese, S.A. Rahman, M.R. Muhamad, Effects of post-thermal annealing temperature on the optical and structural properties of gold particles on silicon suboxide films, Appl. Surf. Sci. 257 (2011) 2208–2213.
[5] U. Kreibig, M. Vollmer, Optical properties of metal clusters, Springer, Berlin, 1995.
[6] M.C. Mathpal, A.K. Tripathi, M.K. Singh, S.P. Gairola, S.N. Pandey, A. Agarwal, Effect of annealing temperature on Raman spectra of TiO_2 nanoparticles, Chem. Phys. Lett. 555 (2013) 182-186.
[7] C.F. Bohren, D.R. Huffman, Absorption and scattering of light by small particles, John Wiley, New York, 1983.
[8] A.D. McFarland, R.P. Van Duyne, Single silver nanoparticles as real-time optical sensors with zeptomole sensitivity, Nano. Lett. 3 (2003) 1057–1062.
[9] Y. Huang, X. Duan, Q.Y. Wei, Directed assembly of one-dimensional nanostructures into functional networks, Sci. 291 (2001) 630-633.
[10] D.A. Schultz, Plasmon resonant particles for biological detection, Curr. Opin. Biotech. 14 (2003) 13-22.
[11] K.L. Kelly, E. Coronado, L.L. Zhao, G.C. Schatz, The optical properties of metal nanoparticles: the influence of size, shape, and dielectric environment, J. Phys. Chem. B. 107 (2003) 668–677.
[12] U. Kreibig, C.V .Fragstein, The limitation of electron mean free path in small silver particles, Z. Phys. 224 (1969) 307-323.
[13] U. Kreibig, L. Genzel, Optical absorption of small metallic particles, Surf. Sci. 156 (1985) 678-700.
[14] C. Noguez, Surface plasmons on metal nanoparticles: the influence of shape and physical environment, J. Phys. Chem. C. 111 (2007) 3806–3819.
[15] S. Link, M.A. El-Sayed, Shape and size dependence of radioactive, non-radioactive and photo thermal properties of gold nanocrystals, Int. Rev. Phys. Chem. 19 (2000) 409-453.
[16] Yu. A. Akimov, K. Ostrikov, E.P. Li, Surface plasmon enhancement of optical absorption in thin-film silicon solar cells, Plasmonics 4 (2009) 107-113.
[17] J. Wang, W.M. Lau, Q. Li, Effects of particle size and spacing on the optical properties of gold nanocrystals in alumina, J. Appl. Phys. 97 (2005) 114303-114310.
[18] J.C. Maxwell-Garnett, Colours in metal glasses and in metallic films, Philos. Trans. R. Soc. London. 203 (1904) 385-420.
[19] E.D. Palik, Handbook of optical constants of solids, Vols. I and II, Academic Press, New York, 1985.
[20] H. Hovel, S. Fritz, A. Hilger, U. Kreibig, M. Vollmer, Width of cluster plasmon resonances: bulk dielectric functions and chemical interface damping, Phy. Rev. B. 48 (1993) 18178-18188.
[21] L.H. Zhou, C.H. Zhang, Y.T. Yang, B.S. Li, L.Q. Zhang, Y.C. Fu, H.H. Zhang, Formation of Au nanoparticles in sapphire by using Ar ion implantation and thermal annealing, Nuc. Instr. Meth. Phys. Res. B. 267 (2009) 58–62.
[22] H.B. Liao, R.F. Xiao, J.S. Fu, P. Yu, G.K. Wong, P. Sheng, Large third-order optical nonlinearity in Au: SiO_2 composite films near the percolation threshold, Appl. Phys. Lett. 70 (1997) 1-3.
[23] I. Tanahashi, Y. Manabe, T. Tohda, S. Sasaki, A. Nakamura, Optical nonlinearities of Au/SiO_2 composite thin films prepared by a sputtering method, J. Appl. Phys. 79 (1996) 1244-1249.
[24] D. Dalacu, L. Martinu, Temperature dependence of the surface plasmon resonance in Au/SiO_2 films, Appl. Phys. Lett. 77 (2000) 4283-4285.
[25] D. Dalacu, L. Martinu, Spectroellipsometric characterization of plasma-deposited Au/SiO_2 nanocomposite films, J. Appl. Phys. 87 (2000) 228-235.
[26] C.H. Kerboua, J.M. Lamarre, L. Martinu, S. Roorda, Deformation, alignment and anisotropic optical properties of gold nanoparticles embedded in silica, Nucl. Instr. Meth. Phys. Res. B 257 (2007) 42-46.
[27] J.M. Lamarre, Z. Yu, C. Harkati, S. Roorda, L. Martinu, Optical and microstructural properties of nanocomposite Au/SiO_2 films containing particles deformed by heavy ion irradiation, Thin Sol. Films 479 (2005) 232-237.
[28] A. Belahmar, A. Chouiyakh, Effect of post-annealing on structural and optical properties of gold nanoparticles embedded in silica films grown by RF-sputtering, Adv. Phys. Theory. Appl. 15 (2003) 38-46.
[29] K.H Jung, J.W. Yoon, N. Koshizaki, Y.S. Kwon, Fabrication and characterization of Au/SiO_2 nanocomposite films grown by radio-frequency cosputtering, Curr. Appl. Phys. 8 (2008) 761–765.
[30] G.Q. Yu, B.K. Tay, Z.W. Zhao, X.W. Sun, Y.Q. Fu, Ion beam co-sputtering deposition of Au/SiO_2 nanocomposites, Phys. E. Low-dim. Sys. Nanostr. 27 (2005) 362–368.
[31] B. Zhuo, Y. Li, S. Teng, A. Yang, Films, fabrication and characterization of Au/SiO_2 nanocomposite films, Appl. Sur. Sci. 256 (2010) 3305–3308.
[32] P. Sangpour, O. Akhavan, A.Z. Moshfegh, M. Roozbehi, Formation of gold nanoparticles in heat-treated reactive co-sputtered Au-SiO_2 thin films, Appl. Surf. Sci. 254 (2007) 286–290.
[33] S. Cho, H. Lim, K.S. Lee, T.S. Lee, B. Cheong, W.M. Kim, S. Lee, Spectro-ellipsometric studies of Au/SiO_2 nanocomposite films, Thin Sol. Films. 475 (2005) 133–138.
[34] M.S. Kennedy, N.R. Moody, D.P. Adams, M. Clift, D.F. Bahr, Environmental influence on interface interactions and adhesion of Au/SiO_2, Mat. Sci. Eng. A. 493 (2008) 299–304.
[35] F. Ruffino, M.G. Grimaldi, C. Bongiorno, F. Giannazzo, F. Roccaforte, V. Raineri, Microstructure of Au nanoclusters formed in and on SiO_2, Superl. Microstruct. 44 (2008) 588–598.
[36] K. Takahiro, S. Oizumi, K. Morimoto, K. Kawatsura, T. Isshiki, K. Nishio, et al, Application of X-ray photoelectro spectroscopy to characterization of Au nanoparticles formed by ion implantation into SiO_2, Appl. Sur. Sci. 256 (2009) 1061-1064.
[37] T. Cesca, C. Maurizio, B. Kalinic, C. Scian, E. Trave, G. Battaglin, P. Mazzoldi, G. Mattei, Luminescent ultra-small gold nanoparticles obtained by ion implantation in silica, Nucl. Instr. Meth. Phys. Res. Sec. B: Beam Inter. Mater. Atoms 326 (2014) 7-10.
[38] M.C. Ferrara, L. Mirenghi, A. Mevoli, L. Tapfer, Synthesis and characterization of sol–gel silica films doped with size-selected gold nanoparticles, Nanotech. 19 (2008) 657 06-65714.
[39] F. Ruffino, C. Bongiorno, F. Giannazzo, F. Roccaforte, V. Raineri, M.G. Grimaldi, Effect of surrounding environment on atomic structure and equilibrium shape of growing nanocrystals: gold in/on SiO_2, Nanosc. Res. Lett. 2 (2007) 240-247.
[40] H.B. Liao, W. Weijia, G.K.L. Wong, Preparation and optical characterization of Au/SiO_2 composite films with multilayer structure, J. Appl. Phys. 93 (2003) 4485-4488.
[41] S. Debrus, J. Lafait, M. May, N. Pinçon, D. Prot, C. Sella, J. Venturini, Z-scan determination of the third-order optical nonlinearity of gold: silica nanocomposites, J. Appl. Phys. 88 (2000) 4469-4475.
[42] N. Pinçon, B. Palpant, D. Prot, E. Charron, S. Debrus, Third-order nonlinear optical response of Au:SiO_2 thin films: Influence of gold nanoparticle concentration and morphologic parameters, Eur. Phys. J. D 19 (2002) 395-402.
[43] A. Belahmar, A. Chouiyakh, Influence of the fabrication conditions on the formation and properties of gold nanoparticles in alumina matrix produced by cosputtering, Int. J. Nano. Mater. Sci. 3 (2014) 16-29.
[44] A.R. West, Solid state chemistry and its applications, Wiley, New York, 1974.
[45] H.R. Doremus, P. Rao, Optical properties of nanosized gold particles, J. Mat. Res. 11 (1996) 2834-2840.
[46] L. Yang, G.H. Li, L.D. Zhang, Effects of surface resonance state on the plasmon resonance absorption of Ag nanoparticles embedded in partially oxidized amorphous Si matrix, Appl. Phys. Lett. 76 (2000) 1537-1539.
[47] F. Moresco, M. Rocca, T. Hildebrandt, T.M. Henzler, Plasmon confinement in ultrathin continuous Ag films, Phys. Rev. Lett. 83 (1999) 2238-2241.
[48] W. Cai, Y. Zhang, J. Jia, L. Zhang, Semiconducting optical properties of silver/silica mesoporous composite, Appl. Phys. Lett. 73 (1998) 2709-2911.
[49] J. Tauc, Amorphous and liquid semiconductors, Plenum, London, 1974.
[50] Z. Aspanut, C.K. Wah, C.S. Kong, R. Ritikos, G.B. Tong, S.A. Rahman, M.R. Muhammad, Fabrication and characterization of co-sputtering Au/SiO_2 thin films prepared by rf magnetron sputtering, Int. Nanoelect. Conf. (INEC) (2010) 970-971.
[51] Z. Cui-Hua, Z. Bo-Ping, S. Peng-Peng, Enhanced nonlinear optical absorption of Au/SiO_2 nano-composite thin films, Chin. Phys. B. 18 (2009) 5539-5543.